Thermal-Induced Wear Mechanisms of Sheet Nacre in Dry Friction

Philippe Stempflé, T. Djilali, Richard Kouitat Njiwa, Marthe Rousseau, Evelyne Lopez, Xavier Bourrat

Thermal - Induced Wear Mechanisms of Sheet Nacre in Dry Friction

Philippe Stempflé[a)], Toufik Djilali[b)], Richard Kouitat Njiwa [c)],

Marthe Rousseau[d)], Evelyne Lopez [e)], Xavier Bourrat [f)]

[a)] Institut FEMTO-ST (UMR CNRS 6174 – Université de Franche Comté – CNRS – ENSMM – UTBM), ENSMM, 26 Chemin de l'Epitaphe, F-25030 Besançon Cedex, France, +33 (0) 3 81 40 27 64, philippe.stempfle@ens2m.fr

[b)] Université de Toulouse, INP/ENIT, Laboratoire Génie de Production, 47 avenue d'Azereix, F-65013 Tarbes, France

[c)] Laboratoire de Science et Génie des Surfaces, Ecole des Mines, Parc de Saurupt, F-54042 Nancy cedex, France

[d)] UMR7561 CNRS - Nancy University, 9 avenue de la forêt de Haye, F-54505, Vandoeuvre les Nancy, France

[e)] Muséum National d'Histoire Naturelle (UMR 5178 CNRS-MNHN), CP26, 43 Rue Cuvier, F-75005 Paris, France

[f)] Université d'Orléans CNRS, ISTO, 1A Rue de la Férollerie, F-45071 Orléans cedex 2, France

Abstract

Sheet nacre is a natural biocomposite with a multiscale structure including a mineral phase of calcium carbonate (97 wt.%) and two organic matrices (3 wt.%). The mineral phase is constituted by an arrangement of $CaCO_3$ biocrystal nanograins (ca 40 nm in size) drowned in an "intracrystalline" organic matrix (4 nm thick) in order to form a microsized flat organomineral aragonite platelet. These platelets are themselves surrounded by an "intercrystalline" organic matrix (40 nm thick) building up a very tough materials. This micro-architecture referred to as "bricks and mortar" nacre structure, is mainly studied for the creation of new organic/inorganic hybrid materials. Currently, little is known about the ncare mechanical behaviour under dynamical loading and more particularly under tribological conditions which involve shocks and thermal effects simultaneously. This paper brings out the thermal-induced damage mechanisms effect on the wear of sheet nacre by the assessment of the thermal component of the friction with a scanning thermal microscope. Results reveal that the mean contact pressure is the main driving force involved in the degradation of the organic constituents. For the lowest mean contact pressure (<0.4MPa), wear is rather weak because the friction-induced thermal component is not sufficient for degrading the organic matrices. In contrast, beyond 0.4 MPa, the friction-induced contact temperature rises up over the melting point of the organic matrices, and may even reach the temperature of the aragonite-calcite phase transformation increasing dramatically the wear of sheet nacre.

Keywords Sheet nacre · Thermal-induced wear mechanisms · Wear debris · AFM · Scanning thermal microscopy

1. INTRODUCTION

Nacre (the pearly internal layer of molluscan shells) is an attractive nanocomposite displaying high mechanical properties, low density, a good biocompatibility and osteogenic properties for human bone

regeneration [1,2]. It is currently studied for both the prosthesis design and the creation of new organic/inorganic bio-inspired hybrid materials [3]. These exceptional properties are generally ascribed to its highly ordered layered *"brick and mortar"* micro-architecture and more particularly to the energy absorption ability of the mortar during crack propagation [4]. In this micro-architecture (fig. 1a), the *"bricks"* (97 wt.%) refer to flat crystals of calcium carbonate in the crystalline form of aragonite (orthorhombic lattice) with a thickness of <500 nm. The *"mortar"* (3 wt.%) is an *"intercrystalline"* thin network (about 40 nm) of a biological organic adhesive mainly composed of silk-fibroin-like proteins and β-chitin. As shown in fig 1b, each aragonite platelet is itself a nanograin-reinforced organic matrix composite consisting of nanosized crystals (mean size about 38 nm) of $CaCO_3$ surrounded by a water soluble *"intracrystalline"* organic phase (≅ 4 nm) organised as foam [5]. Recently, friction and wear behaviour of sheet nacre were studied respectively in dry friction [6,7] and liquid medium [7]. They have shown that:

- The environment strongly influences the wear mechanisms of nacre by means of various physicochemical interactions on the water-soluble *"intracrystalline"* organic phase;
- the energy absorption ability of the mortar is drastically reduced in presence of nanoshocks generated during friction by the dynamic solicitations; and
- unfortunately some friction-induced damage mechanisms involving thermal effects remain largely misunderstood.

The aim of the present paper is to bring out these thermal-induced damage mechanisms effects on nacre wear from the assessment of the thermal component of friction involved by the degradation of the organic matrices.

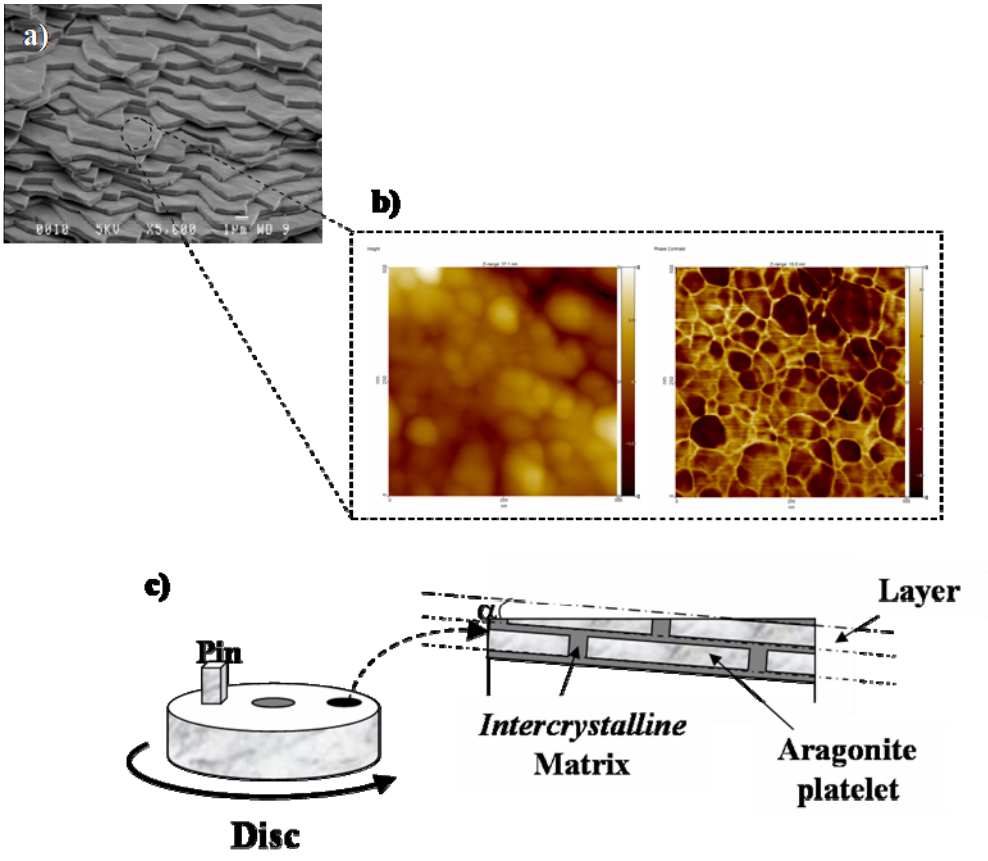

Figure 1: a) "Bricks and mortar" microarchitecture of sheet nacre revealing the "intercrystalline" organic phase: b) Each platelet is constituted by nanosized $CaCO_3$ grains surrounded by an "intracrystalline" organic phase, and c) Schematic cross section of the friction surface ($\alpha \approx 8°$)

2. EXPERIMENTAL

2.1 Samples

Samples are made of sheet nacre extracted from giant oyster *Pinctada maxima* [6,7]. They are polished more or less parallel to the aragonite platelets (size: 5µm, thickness: 400 nm, Ra: 14.5 ± 0.6 nm) (fig 1c). The average size of the nanograins assessed by AFM image analysis is 38 ± 21 nm. The thickness of the *"intracrystalline"* matrix is about 4 nm and its average volume fraction V_m – evaluated for a covered area about 10 μm^2 – is about 12% in 2D corresponding to 4.2% in 3D. This value is close to the one obtained by chemical extractions [8]. The Hardness H, the density ρ, the thermal conductivity K and the specific heat σ of samples are respectively 7.8 ± GPa [6], 2830 $kg.m^3$, 3 ± 2 $W.m^{-1}K^{-1}$ and 1350 ± 150 $J.kg^{-1}K^{-1}$ [9].

2.2 Tribological Tests

The experimental device is constituted by a *pin-on-disc* tribotester manufactured by *CSM Instruments* (*Switzerland*) [6,7]. Tests are carried out at ambient air and room temperature in dry conditions by repeated friction of a 3.5 mm square shaped pin of nacre against the surface of a polished disc of nacre (∅ 44 mm). The normal load (F_n) varies from 1N to 15N (corresponding to a mean contact pressure of 0.1 – 1.2 MPa). The sliding speed and length are respectively, 10 $mm.s^{-1}$ and 100 m. The wear rate of pin and disc are determined after 100 m of sliding from the weight of the material lost during the test, with a precision of 10^{-4} g. According to the previous mechanical [6] and thermal properties of the samples [9], and the expected average real contact area computed from the experimental conditions [10], the value of the Peclet number L- introduced as a criterion allowing the differentiation between various speed regimes [11]- is very weak (<0.18). Hence, the situation during the tribological tests closely approximates to steady state conduction.

2.3 Near Field Microscopy

2.3.1 Atomic Force Microscopy

Topography is assessed using an AFM *Dimension 3000* connected to a *Nanoscope IIIa* electronic controller (*Digital Instruments USA*) [5,7]. Its spatial and vertical resolutions are lower than 1 nm and the field depth is in-between 100 nm and 100 µm. Maps were achieved at high resolution (512×512 pixels) using an intermittent contact mode (so-called *TappingMode™*). The silicon nitride probe displays a tip rounding lower than 10 nm. The work frequency, the stiffness and the cantilever amplitude are respectively: 270 kHz, 42 Nm^{-1} and 25 nm. Depending on the size of the images (between 0.25 μm^2 and 25 μm^2) the scanning rates varies from 1 $\mu m.s^{-1}$ to 2.4 $\mu m.s^{-1}$.

2.3.2 Scanning Thermal Microscopy

The local thermal properties of the samples are assessed with a SThM (*TA Instruments µTA 2990* with a *TA Instruments controller TA 5300, New Castle, DE*) which is an analytical system that combines the high resolution visualization and positioning methods of scanning probe microscopy with the technology of thermal analysis [12,13]. The standard AFM probe is replaced by a thermal probe made from a Wollaston wire (5µm diameter platinum-10% rhodium wire enclosed in a silver sheath) which allows the acquisition of the surface contact area temperature, and simultaneously acts as a highly localized heater [12-14]. The vertical deflection of the assembly is monitored by a light pointing technique. The spring constant is 10 $N.m^{-1}$. The constant current setpoint and the z-setpoint are 1 mA and 50 V, respectively. The probe rate is 100 $\mu m.s^{-1}$. This latter is sufficiently weak so that the heat transfer regime stays in the steady state conduction as in the tribological tests [11, 15]. The spatial resolution and the thermal sensitivity are, respectively, about 100 nm and 1°C [15]. Calibration of the SThM is made by using three reference polymeric samples [14]: PAI TORLON (T_g = 285°C), PEI ULTEM1000 (T_g = 215°C), PPS (T_g = 94.4°C, T_f = 281°C).

3. RESULTS AND DISCUSSION

3.1 Friction behaviour variation *vs.* sliding length

The dissipated power by friction is given by $P = \mu F_n v$ where μ is the friction coefficient, Fn the normal load and v the sliding velocity [16]. Figure 2 shows its variations in function of the sliding length for various normal loads. The curves are highly disturbed due to local nanoshocks induced by the natural structure of sheet nacre [6]. After a run-in period, the deduced Coulomb's friction coefficient is about 0.44 ± 0.02 (Fig. 3).

3.2 Wear rate variation *versus* normal load

The plot of the wear rate (μg.m^{-1}) of the pin and the disc *versus* the normal load are shown in Fig. 4.

- For the pin, the wear rate is very weak and rather insensitive to the normal load.
- For the disc, up to 5N, the wear rate steadily increases with values greater than that of the pin. Above a normal load of 5N (corresponding to a mean contact pressure of 0.4 MPa), the wear rate dramatically rises whereas, in the same time, the friction coefficient stays stable (Fig. 3);

Such behaviour is often observed when a dissymmetry in temperature or in the exposure time to the external environment of contacting bodies occurred [7]. Considering the heat transfer regime involved withing the contact (close to the steady state conduction), there is enough time for the contact temperature distribution to be established in the stationary body – *i.e* the pin [11]. Hence, the pin contact temperature stays constant in contrast to the one of the disc which undergoes a thermal cycling. Thus, the difference between the two wear rates could be due to a thermal dissymmetry between the *pin* and the *disc*. In order to check this assumption we first have to analyse the damage of the friction track.

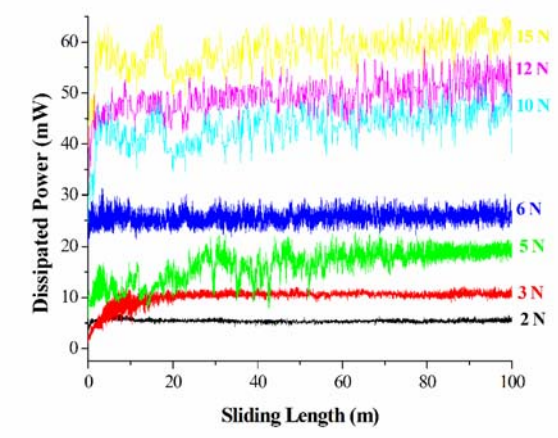

Figure 2: Variation of the dissipated power by friction versus sliding length for various normal loads

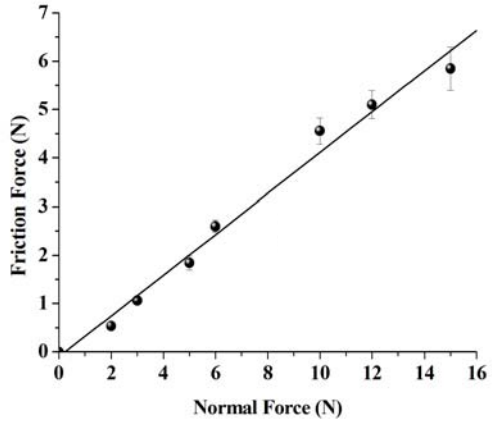

Figure 3: Determination of the coefficient of friction of sheet nacre by the slope of Ft = f (Fn)

3.3 Wear mechanisms

3.3.1 Observation of the Friction Track Damage

Figure 5 shows a typical AFM view of the friction track after 100 m of sliding. The worn surface is strongly degraded by parallel cracks aligned across the structure of sheet nacre. It is clear that fracture occurs within the platelets itself and involves the fracturing of the *"intracrystalline"* organic matrix. In a recent work, we have demonstrated that this damage is a kind of crumbling of the aragonite platelets due to friction-induced nanoshocks [6]. For low loads (<5 N), this wear mechanism rationalises the formation of wear nanodebris having an average size of 44 nm very close to the one of the biocrystal nanograins [7]. However, this wear mechanism does not explain the abrupt rise of the wear rate when the load is increased beyond 5 N (fig.4). If nanoshocks phenomena are likely always involved at highest pressures (as supposed with the dashed line on the Fig. 4), another mechanism is probably superimposed for increasing the slope of the wear rate.

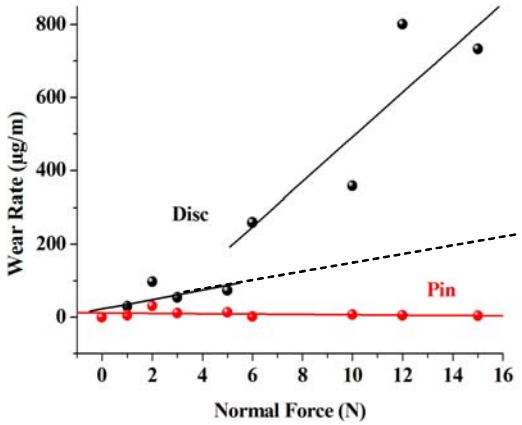

Figure 4: Variation of the wear rate with the normal load.

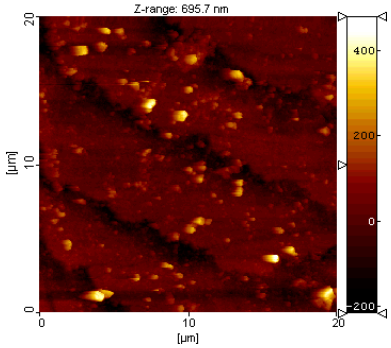

Figure 5: Typical AFM view of the friction track revealing the crumbling of the aragonite platelets by the presence of nanoshocks

3.3.2 Wear debris

Wear debris generated under various normal loads are then observed with X-Ray diffraction and compared to the original spectrum of aragonite [17]. As shown in the Fig. 6, the intensity of the *calcite peak* (expected at 34.28°) – *i.e* the other crystallographic form of $CaCO_3$ – gradually increases when the normal load increases from 5 N to 15 N. This result is also confirmed by observations of the wear debris using cathodoluminescence (Fig.7). This technique is particularly sensitive to any modification of the lattice. Thus, for the calcium carbonate, the aragonite structure (*orthorhombic lattice*) emits in the *blue/green* whereas the calcite (*rhombohedric lattice*) emits in the *yellow*. As shown in Fig 7, the most coarse debris present a transition between the aragonite and the calcite (*green* grains with *yellow* spots) whereas the smallest grains appear in *yellow* because they are completely transformed into calcite. In addition, cathodoluminescence investigations carried out on the friction track reveal that the discontinuous tribo-layers -generated for the highest loads- are mainly constituted by the calcite form of $CaCO_3$. According to our previously work [7], in dry friction the pin is almost entirely covered by a strongly bonded tribolayer. Hence, the weak wear rate of the pin –as observed in Fig.4- could be simply explained by the protective effect of this strongly adhesive calcite tribolayer vovering the pin. Anyway, these results prove that the mineral component of the wear debris can undergo a phase transformation within the contact.

As shown in the Fig 8 and in [8], the irreversible transformation of calcium carbonate from aragonite to calcite generally occurs when the temperature reaches 470°C. However, these high temperatures can be briefly reached at the level of the microscopic asperities within the contact. This is because the real contact pressure can reach several GPa [11, 18]. In our case, the real contact area is about a thousandth of the apparent area (3.5 × 3.5 mm2) [10, 19]. Referring to [11, 18, 20], the contact temperature is mainly controlled by the normal load when the sliding speed is constant. Since thermal-induced structural changes of the mineral phase are observed during high load tribological tests, the temperatures which drive the melting of the organic matrices should be reached for the lower normal loads – somewhere in-between 2 N to 15 N.

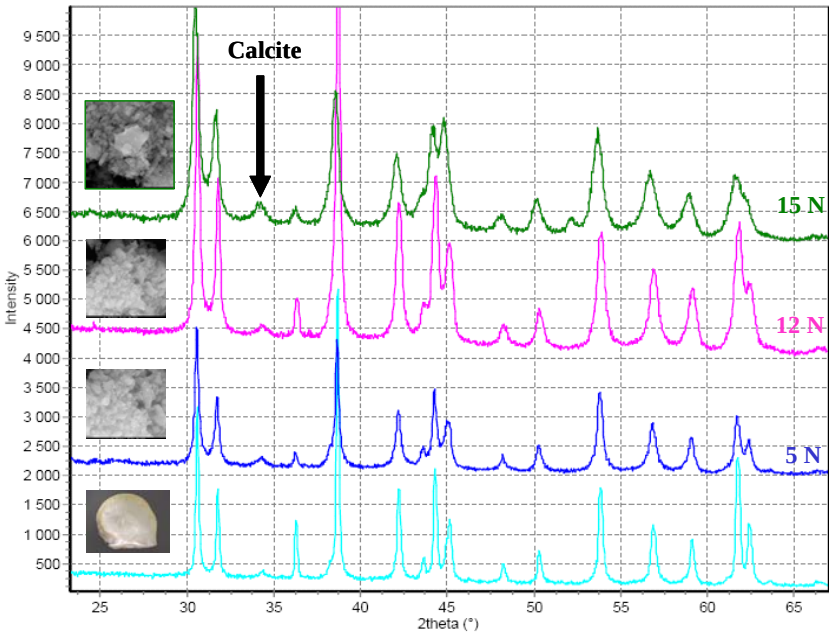

Figure 6: X-ray diffraction spectra of wear debris generated under various normal loads

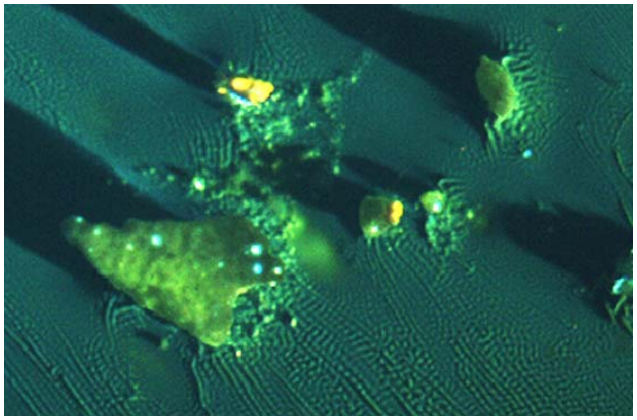

Figure 7: Typical cathodoluminescence view of the wear debris deposited on epoxy resin. Aragonite appears in green (dark zone) whereas calcite appears in yellow (bright points)

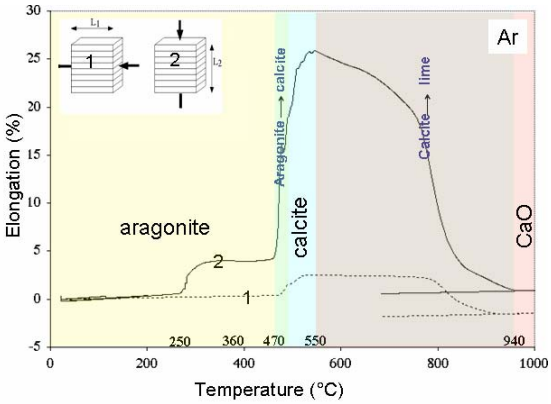

Figure 8 : TMA plot of nacre blocks up to 1000°C under argon (1) sensor parallel to the plane and (2) perpendicular to the tablet stack [8]

3.4 Power Dissipated by Thermal Assessment

Since 98% of the power dissipated by friction is lost by the thermal way [11, 18], SThM can be used to link the contact temperature with the thermal power dissipated at the level of the micro-asperity. Indeed, the probe of the SThM properly simulates the thermal dissipation of the local micro-asperity. During the imaging process, the tip is in direct contact with the surface. Changes in thermal conductivity across the surface result in a different heat flow between the tip and sample. Hence, changes in this property can be acquired by measuring the power level which is necessary to maintain the tip-temperature at a constant value. Thus, contrast in topography, in thermal conductivity (*e.g.* Fig. 10) and/or diffusivity across the surface of the sample are simultaneously acquired [12-15]. Figure 9a, b shows, respectively, the results of 15 experimental tests:

- The µDTA curve (Fig. 9a) displays the power level necessary to keep the heating rate constant. The power is measured relatively to a reference probe. Hence, this curve reveals the relation between the contact temperature and the dissipated power;

- The µTMA curve (Fig.9b) simultaneously displays the change of the vertical displacement of the cantilever as a function of the contact temperature. The continuous rise of the sensor with the contact temperature corresponds to the thermal expansion of the nacre sample. However, beyond 200°C, sensor jumps are also observed with amplitude a high as 250 to 500 nm.

According to the work of Bourrat *et al* [8], thermal expansion of sheet nacre in the slot of temperature 200°C to 350°C can be attributed to the melting of the organic matrices (see Fig. 8 curve 2). Thus, these thermal-induced jumps show that the platelets can come unstuck when the organic phase is degraded. Since the organic matrices ccontain mainly proteins and chitin the term “degraded” is probably much more suitable than the term “melted” because the degradation of the organic matrices does not imply a reversible process in contrast to the *melting*. In addition, µDTA plot (Fig. 9a) reveals that the minimum power for degrading the organic phase is about 20 mW. In order to check this assumption, Fig.10a, b shows the typical SThM views of the same area observed at 200°C, respectively, before (Fig. 10a) and after heating at 350°C (Fig. 10b). After heating at 350°C (corresponding to a power about 35 mW), the organic matrix clearly vanished. In addition, the power level necessary to keep the temperature at 200°C is reduced of about 2 mW due to the disappearance of the organic phase's additional thermal resistance.

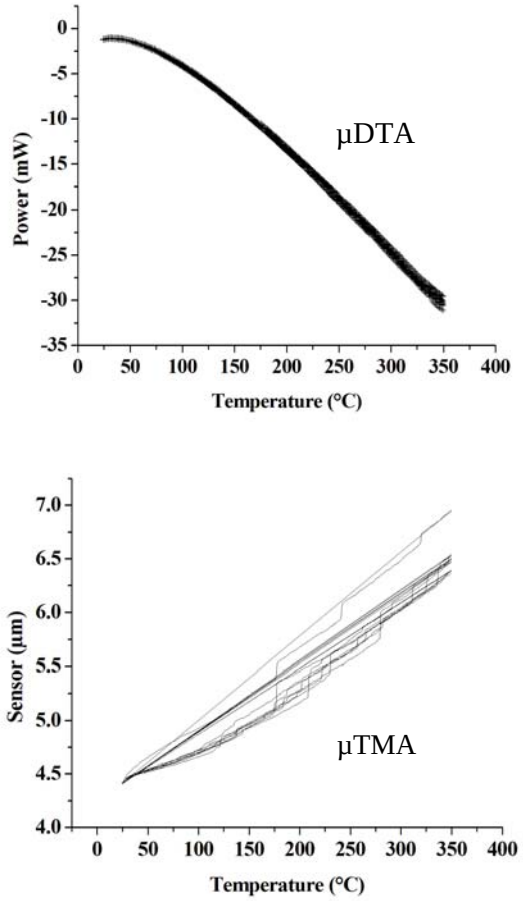

Figure 9 a) µDTA plot: dissipated power versus contact temperature and b) µTMA cantilever displacement versus contact temperature

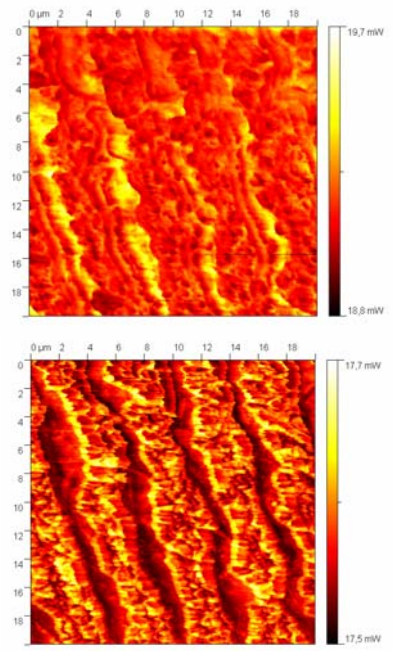

Figure 10: Typical SThM views of the same area observed at 200°C a) before and b) after heating at 350°C

3.5 Friction-induced thermal behaviour

In order to link the previous observations with the tribological ones, the average contact temperature at the level of the micro-asperities within the tribological contact can be estimated – for each normal load – by comparing the respective power level given by the µDTA graph (Fig 9a) with the thermal power dissipated by friction during the tribological tests. This latter is assumed to be 98% of the friction power displayed in the fig. 2. Consequently, the multi-asperity contact temperature can be determined in function of the contact pressure – *i.e* the normal load. These results show that:

- For the low contact pressures (<0.4 MPa corresponding to 5 N), the friction-induced thermal component is not sufficient for melting the organic matrices (17 mW, T_c < 210°C). According to Madhusudana [20], the greater part of the thermal power is lost in the gas gap because the contact pressure is lower than 10^{-4} H (with H the hardness of the sample). Hence, in this case, the wear is mainly controlled by the presence of nanoshocks [6];

- When the contact pressures are greater than 0.4 MPa (*i.e* normal load higher than 6 N), the friction-induced contact temperature rises up to the melting point of the organic matrices (*e.g.,* for 6N, 24.5mW, $T_c \cong 282$°C). In this case, the greater part of the thermal power is lost by conduction across the gas filling the voids between the actual contact spots and across the spots [15, 19, 20] ;

- The aragonite-calcite phase transformation is observed within the contact when the contact pressure is higher than 1 MPa (*i.e.,* normal load higher than 11N). Extrapolation of the curve gives: 49 mW and $T_c \cong 508$°C ;

Thus, in these two latter cases, wear becomes a combination of nanoshocks and thermal effects – combining degradation of the organic matrices, and friction-induced phase transformation of the mineral phase. This combination explains both the abrupt change in the wear rate with the contact pressure beyond 0.4 MPa and also the dissymmetry between the wear rate of the pin and the one of the disc.

4. CONCLUSION

The aim of this paper was to bring out the effect of the thermal-induced damage mechanisms on the wear of nacre by using the assessment of the thermal component of the friction which is involved in the degradation of the organic matrices. For this purpose, the SThM is used for controlling the thermal power really injected within the sample. The latter is then compared with the power dissipated by friction during the tribological tests. Results reveal that:

- When the mean contact pressure is lower than 0.4MPa, the friction-induced thermal component is not sufficient for degrading the organic matrices. Wear is mainly controlled by the presence of shocks.

- When the mean contact pressure is increased beyond 0.4 MPa, the friction-induced contact temperature rises up, over the degradation point of the organic matrices, and may even reach the temperature of the *aragonite-calcite* phase transformation: the wear is dramatically increased.

- The weak wear rate of the pin can be attributed to a protective effect of the strongly adhesive calcite *tribolayer* covering the pin.

ACKNOWLEDGEMENTS

Philippe Penhoud (Orleans University) and Vincent Barbin (Reims University) are acknowledged for X-ray and cathodoluminescence analyses, respectively. The authors thank Tahiti Perles Company and its Chairman Robert Wan for having supplied them with the best nacre quality.

REFERENCES

1. Lopez, E., Vidal, B., Berland, S., Camprasse, S., Camprasse, G., Silve, C.: Demonstration of the capacity of nacre to induce bone formation by human osteoblasts maintained in vitro. Tissue Cell 24, 667–679 (1992). doi:10.1016/0040-8166(92)90037-8
2. Carlson, J., Ghaey, S., Moran, S., Tran, C.A., Kaplan, D.L.: Biological materials in engineering mechanisms. In: Bar-Cohen, Y. (ed.) Biomimetics, Biologically Inspired Technologies, pp. 365–379. CRC Taylor & Francis, Boca Raton, FL, (2006). ISBN-10: 0849331633
3. Munch, E., Launey, M.E., Alsem, D.H., Saiz, E., Tomsia, A.P., Ritchie, R.O.: Tough, bio-inspired hybrid materials. Science 322, 516–520 (2008). doi:10.1126/science.1164865
4. Okumura, K., de Gennes, P.G.: Why is nacre strong? Elastic theory and fracture mechanics for biocomposites with stratified structures. Eur. Phys. J. E 4, 121–127 (2001). doi:10.1007/s101890170150
5. Rousseau, M., Lopez, E., Stempfle´, P., Brendle´, M., Franke, L., Guette, A., Naslain, R., Bourrat, X.: Multiscale structure of sheet nacre. Biomaterials 26(31), 6254–6262 (2005). doi:10.1016/j.biomaterials.2005.03.028
6. Stempfle´, P., Pantale´,O.,KouitatNjiwa,R.,Rousseau, M., Lopez, E., Bourrat, X.: Friction-induced sheet nacre fracture: effects of nanoshocks on cracks location. Int. J. Nanotechnol. 4(6), 712–729 (2007)
7. Stempfle´, Ph., Brendle´, M.: Tribological behaviour of nacre—influence of the environment on the elementary wear processes. Tribol. Int. 39, 1485–1496 (2006)
8. Bourrat, X., Franck, L., Lopez, E., Rousseau, M., Stempfle´, P., Angellier, M., Alberic, P.: Nacre biocrystal thermal behaviour. CrystalEngComm 9, 1205–1208 (2007). doi:10.1039/b709388h
9. Cambridge Engineering Selector InDepth, v. 3.1, Granta Design Limited CD ROM (2000). http://www.grantadesign.com
10. Mate, C.M.: Tribology on the Small Scale. Oxford University Press, Oxford, 400 p (2007). ISBN-10: 0198526784
11. Stachowiak, G.W., Batchelor, A.W.: Engineering Tribology. Butterworth-Heinemann Ltd, 744 p (2002). ISBN-10: 0750673044
12. Pollock, H.M., Hammiche, A.: Micro-thermal analysis: techniques and applications. J. Phys. D Appl. Phys. 34(R23–R53),
1–41 (2001)
13. Ha¨ßler, R., zur Mu¨hlen, E.: An introduction to lTA and its application to the study of interfaces. Thermochim. Acta 361,
113–120 (2000). doi:10.1016/S0040-6031(00)00552-9
14. lTA 2990 Operator's Manual, Calibrating the lTA 2990, pp. 113-129 (2003)
15. Gome`s, S., Trannoy, N., Grossel, P., Depasse, F., Bainier, C., Charraut, D.: D.C. scanning thermal microscopy: characterisation
and interpretation of the measurement. Int. J. Therm. Sci. 40, 949–958 (2001). doi:10.1016/S1290-0729(01)01281-9
16. Sherge, M., et al.: An energetic approach to friction, wear and temperature. Wear 257, 124–130 (2004). doi:10.1016/j.wear.
2003.10.010
17. Balmain, J., Hannoyer, B., Lopez, E.: FTIR and X-ray diffraction analyses of mineral and organic matrix during heating of mother
of pearl (Nacre) from the shell of the mollusc Pinctada maxima. J. Biomed. Mater. Res. Appl. Mater. 48(5), 749–754 (1999).
doi:10.1002/(SICI)1097-4636(1999)48:5\749::AID-JBM22[3.0.CO;2-P
18. Vick, B., Furey, M.J.: A basic theoretical study of the temperature rise in sliding contact with multiple contacts. Tribol. Int. 34,
823–829 (2001). doi:10.1016/S0301-679X(01)00082-2
19. Stempfle´, Ph., et al, to be published
20. Madhusudana, C.V.: Thermal Contact Conductance. Springer Verlag, New York, 165 p (1998). ISBN-10: 0387945342